Characterization of ZO-1, a Protein Component of the Tight Junction from Mouse Liver and Madin-Darby Canine Kidney Cells

James Melvin Anderson,*‡ Bruce R. Stevenson,‡ Lynne A. Jesaitis,§ Daniel A. Goodenough,§ and Mark S. Mooseker‡

*Department of Medicine and Liver Center, Yale School of Medicine and
‡Department of Biology, Yale University, New Haven, Connecticut 06511-8112; and
§Department of Anatomy and Cell Biology, Harvard Medical School, Boston, Massachusetts 02115

Abstract. ZO-1, originally identified by mAb techniques, is the first protein shown to be specifically associated with the tight junction. Here we describe and compare the physical characteristics of ZO-1 from mouse liver and the Madin-Darby canine kidney (MDCK) epithelial cell line. The ZO-1 polypeptide has an apparent size of 225 kD in mouse tissues and 210 kD in canine-derived MDCK cells as determined by SDS-PAGE/immunoblot analysis. ZO-1 from both sources is optimally solubilized from isolated plasma membranes by either 6 M urea or high pH conditions; partial solubilization occurs with 0.3 M KCl. The nonionic detergents, Triton X-100 and octyl-β-D-glucopyranoside, do not solubilize ZO-1. These solubility properties indicate that ZO-1 is a peripherally associated membrane protein. ZO-1 was purified to electrophoretic homogeneity from [^{35}S]methionine metabolically labeled MDCK cells by a combination of gel filtration and immunoaffinity chromatography. Purified ZO-1 has an $s_{20,w}$ of 5.3 and Stokes radius of 8.6 nm. These values suggest that purified ZO-1 is an asymmetric monomeric molecule. Corresponding values for mouse liver ZO-1, characterized in impure protein extracts, were 6 $s_{20,w}$ and 9 nm. ZO-1 was shown to be a phosphoprotein in MDCK cells metabolically labeled with [^{32}P]orthophosphate; analysis of phosphoamino acids from purified ZO-1 revealed only phosphoserine. ZO-1 epitope number was determined by Scatchard analysis of competitive and saturable binding of two different ^{125}I-mAbs to SDS-solubilized proteins from liver and MDCK cells immobilized on nitrocellulose. Saturation binding occurs at 26 ng mAb/mg liver and 63 ng/mg of MDCK cell protein. This is equivalent to 30,000 ZO-1 molecules per MDCK cell assuming a single epitope/ZO-1 molecule.

THE tight junction is a plasma membrane structure that seals together the perimeters of polarized epithelial cell monolayers and provides the paracellular barrier necessary to maintain vectoral secretion, absorption, and transport. The paracellular conductance, as well as the molecular size and charge selectivity established by the junction, varies between tissues and evidence has been presented that the junction may be under physiologic regulation within a single tissue (for reviews see references 6, 23). There is also evidence that the tight junction restricts the movement of membrane lipids (28) and proteins (22) between the apical and basolateral membrane domains, although its role in establishing cell polarity is still controversial (2, 30). It is characteristically positioned as the apical-most member of the lateral membrane junctional complex, which includes adherens junctions, desmosomes, and gap junctions (8). When viewed by thin section electron microscopy, the tight junction appears as a set of irregularly spaced points of cell-cell membrane apposition. Freeze-fracture replicas of the tight junction reveal a band of variably spaced and anastomosing fibrils that circumscribe the cell at the apical-basolateral border (10). These fibrils appear to correspond to the points of cell-cell contact and their number is proportional to the transepithelial electrical resistance of the epithelium (4, 18).

An understanding of the molecular basis for variability and regulation of the tight junction has been impeded by the absence of specific biochemical markers. Our laboratories have recently reported, through use of monoclonal antibody techniques, identification of ZO-1, the first protein uniquely associated with the tight junction (25). ZO-1 from mouse tissues has an apparent molecular mass of 225 kD on immunoblots and is localized, in an uninterrupted manner, along the junctional complex region. At the ultrastructural level, using immunogold labeling, ZO-1 appears concentrated near the cell-cell contact points of the junction. We have now charac-

terized the physical and biochemical properties of ZO-1 from both mouse liver and the Madin-Darby canine kidney (MDCK) cell line.

Materials and Methods

Reagents were obtained from Sigma Chemical Co. (St. Louis, MO) unless otherwise stated.

Monoclonal Antibodies

Detailed methods for production of the mAb, R26.4C, produced against a canalicular-enriched membrane fraction from mouse liver have been described previously (25). The present study also uses two additional anti-ZO-1 mAbs, R40.40D3 and R40.76, produced by separate but identical fusion protocols. Because the species source of immunogen in all cases was mouse, immunizations were done in rats and fusions performed with the mouse myeloma line P3X63 Ag8U.1 (CRL 1597; American Type Culture Collection, Bethesda, MD). Based on subunit molecular masses (~56 kD and 27 kD) and Stokes radii observed on gel chromatography, all three mAbs are of the IgG class. All react specifically with a single 225-kD protein, ZO-1, on immunoblots of mouse tissues and localize exclusively to the junctional complex region in MDCK cells and mouse tissues by indirect immunofluorescent staining (data not shown). Monoclonal antibodies were routinely collected from culture supernatants of hybridomas grown in RPMI-1640 (KC Biologicals Inc., Lenexa, KS) containing Nutridoma-SP (Boehringer Mannheim Biochemicals, Indianapolis, IN). Conditioned culture media used directly for staining immunoblots were made 0.2% in NaN_3, adjusted to pH 8.0, and stored frozen or at 4°C. mAbs were also produced by growth of hybridomas in mouse ascites by standard techniques (11); however, athymic mice (Life Sciences, St. Petersburg, FL) were used to avoid rejection of the crossed-species (rat-mouse) hybridomas. Antibodies used for production of mAb-immunoaffinity matrix were purified from tissue culture supernatants by precipitation with $(NH_4)_2SO_4$ (40% saturated). The precipitated mAbs were dialyzed against PBS (150 mM NaCl, 20 mM NaH_2PO_4, pH 7.4) and were 90% pure by SDS-PAGE. Antibodies for radiolabeling were further purified to homogeneity by affinity chromatography on rabbit anti-rat IgG Sepharose (No. 7613-0081; Cappel Laboratories, Cochranville, PA). Protein bound in PBS was eluted with 150 mM NaCl, 0.1 M glycine, pH 3.0, collected, and neutralized in tubes containing 200 mM Tris-base, pH 10.0.

Cell Cultures and Metabolic Labeling

Hybridomas were maintained as previously described (25). MDCK cells were of the low resistance type II strain (3) and were grown on plastic tissue culture plates (Lab-Tek Products, Westmont, IL) in DME (KC Biologicals Inc.), supplemented with 2 mM glutamine, 10% FBS, and penicillin-streptomycin. The cells were passaged twice weekly.

Confluent monolayers were used for all metabolic labeling protocols. For ^{32}P labeling, cells on 10-cm-diam plates were first depleted of phosphate by two 5-min incubations in 130 mM NaCl, 4.7 mM KCl, 1.2 mM $MgCl_2$, 1.6 mM $CaCl_2$, 5 mM dextrose, 30 mM Hepes, pH 7.4. Labeling was done in 10 ml/plate of the same buffer supplemented with 40–100 μCi/ml of neutralized [^{32}P]orthophosphate (0.8 mCi/ml; Amersham Corp., Arlington Heights, IL). Specific activity of TCA-precipitable whole cell protein equilibrated at between 3.5 and 4.5 h at which time cells were used. ^{35}S labeling was done in cultures depleted of methionine by two 30-min preincubations in methionine-free DME (KC Biologicals) supplemented with 10% dialyzed FBS. Fresh methionine-free media containing 40–50 μCi/ml of [^{35}S]methionine (>8,000 Ci/mmol; Amersham Corp.) was added for 12–16 h. Cells were then washed three times on ice with PBS and processed.

Tissue Preparation for ZO-1 Molecular Mass Comparison

CD-1 mice were euthanized by cervical dislocation and organs were quickly removed and washed in cold PBS. Liver and kidney tissues were weighed and dounced in 10 vol (wt/vol) of 1 mM $NaHCO_3$ containing 2 mM phenylmethylsulfonyl fluoride (PMSF). Stomach and colon mucosal epithelia were scraped off of underlying tissue and homogenized in the same manner. Protein from all tissues was precipitated with 5% TCA, pelleted by centrifugation, and solubilized at the same wt/vol ratio in SDS-PAGE sample buffer. Proteins were subjected to electrophoresis on 7.5% acrylamide/0.2% methylene bisacrylamide gels. Molecular masses were determined from a plot of log M_r vs. migration distance by comparison with standards of rabbit skeletal myosin (200 kD) and the two subunits of human spectrin (assumed to be 240 and 220 kD).

Cell Fractionation and ZO-1 Extraction

Mouse Liver. A canalicular-enriched (tight junction-containing) membrane fraction from mouse liver was prepared as previously described (24). All steps were done on ice or at 4°C. After fractionation by sucrose gradient centrifugation, membranes at the 25:41% interface were collected and diluted with 10 vol of buffer A (10 mM Tris-HCl, pH 8.0, 1 mM EDTA, 1 mM dithiothreitol [DTT]) containing the following protease inhibitors: 2.5 μg/ml leupeptin, 0.5 μg/ml chymostatin and pepstatin, and 0.02 TIU of aprotinin. Membrane samples used for extraction experiments were washed twice in buffer A by pelleting at 10,000 *g* for 20 min, were resuspended in 9 vol of buffer A containing specific extraction agents (e.g., urea, KCl), and membranes were separated from solubilized proteins by centrifugation at 100,000 *g* for 1 h. The resultant pellets and supernatants were analyzed by SDS-PAGE and immunoblotting. Specific extraction conditions are indicated in Results.

MDCK Cells. Plasma membrane-enriched fractions from confluent monolayers of MDCK cells were prepared as described previously using dounce homogenization to break cells followed by several differential centrifugation steps (25). Membranes were washed and extracted by the protocol outlined for liver membranes above.

For immunoaffinity purification of ZO-1, membranes were further purified by sedimentation on a single-step (10:50%) sucrose gradient spun at 100,000 *g* for 60 min (SW 41 rotor) in 10 mM imidazole, pH 7.4, 1 mM EDTA, 0.2 mM PMSF. Membranes at the 10:50% interface were free of visible nuclear contamination, as determined by light microscopy. ZO-1 was extracted from membranes, as indicated in the text, and the insoluble membrane fraction was removed by sedimentation at 100,000 *g* for 1 h. Soluble protein was fractionated by gel permeation chromatography on S-400 (1.5 × 48.0 cm or 2.5 × 70.0 cm columns; Pharmacia Fine Chemicals, Piscataway, NJ). ZO-1-containing fractions were located by immunoblot analysis of column fractions.

Immunoaffinity Purification of ZO-1

Immunoaffinity matrix was prepared by coupling purified R26.4C mAb to cyanogen bromide-activated Sepharose (Pharmacia Fine Chemicals) by the manufacturer's suggested protocol. Typical product contained 0.6–0.7 mg of mAb/ml of hydrated beads and was stored in PBS, 0.05% NaN_3 at 4°C.

ZO-1 was immunoprecipitated directly from solubilized whole MDCK cells by the following protocol. All steps were carried out at 0–4°C. Confluent monolayers of cells were washed on plates with PBS containing 0.2 mM PMSF, scraped, and collected by centrifugation at 1,000 rpm in a clinical centrifuge. ZO-1 was extracted from these cells by vortexing in 800 μl per plate of extraction buffer (6 M urea, 0.1% Triton X-100 [TX-100],[1] 10 mM Tris, pH 8.0, 1 mM DTT, 5 mM $MgCl_2$, 5 mM EGTA, 150 mM NaCl, and 0.2 mM PMSF). Insoluble material, which contained no immunoreactive ZO-1, was removed by centrifugation at 15,000 *g* for 10 min. 100 μl of supernatant was diluted with 9 vol of extraction buffer without urea and 20 μl of R26.4C-Sepharose was added and mixed by rotation for 4 h. Bound ZO-1 was pelleted in 1.5-ml tubes in an Eppendorf microfuge and washed extensively with 150 mM NaCl, 1 M urea, 0.1% TX-100, 1 mM DTT, and 10 mM Tris, pH 8.0. Before SDS-PAGE, beads were washed a final time in 10 mM Tris, pH 8.0, and extracted into an equal vol of 2× concentrated SDS-PAGE sample buffer (1× is 1% SDS, 1% mercaptoethanol, 5% glycerol, 5 mM Tris, pH 6.8) with heating to 100°C for 3 min. ZO-1 for hydrodynamic studies was purified as above and then removed from the beads in 4 vol of buffer containing 150 mM NaCl, 4 M urea, 10 mM Tris, pH 7.4, and 1 mM DTT.

Hydrodynamic Characterization

The sedimentation coefficient, $s_{20,w}$, of ZO-1 was estimated by rate-zonal sedimentation on linear 5–20% sucrose gradients in an SW 41 rotor by the method of Martin and Ames (19). ZO-1 eluted from the immunoaffinity matrix was diluted with 4 vol of gradient buffer without sucrose before application to the gradient. Centrifugation was performed with 400-μl samples applied to 11.6-ml gradients in 150 mM NaCl, 20 mM Tris, pH 7.4, and 1 mM

1. *Abbreviation used in this paper*: TX-100, Triton X-100.

DTT for 20 h at 40,000 rpm and at 4°C. 0.6-ml fractions were collected and the positions of marker proteins determined by SDS-PAGE. The position of ZO-1 was determined by immunoblot analysis; in the case of pure ^{35}S-labeled protein, present at a level below detection by immunoblotting, its position was determined by scintillation counting of whole gradient fractions.

Stokes radius, R_a, was estimated by chromatography of ZO-1–containing samples and marker proteins on a Sephacryl S-400 gel filtration column (1.5 × 48.0 cm) eluted at 4°C with 8 ml/h of the same buffer used for sedimentation studies (1). Void and included column volumes were determined by the positions of Blue Dextran and potassium ferrocyanate, respectively. ZO-1 was located by immunoblotting or scintillation counting. A plot of Stokes radii of standard proteins vs. erf^{-1} ($1\text{-}K_{av}$) was fit by linear least-squares regression and R_a of ZO-1 extrapolated (1).

Phosphoamino Acid Analysis

Confluent cultures of MDCK cells were metabolically labeled for 4 h with [^{32}P]orthophosphate and ZO-1 collected by immunoprecipitation as described above. Immunoprecipitated proteins were subjected to SDS-PAGE. ZO-1, located by autoradiography of dried gels, was cut from the gel and rehydrated into 50 mM NH_4HCO_3. All subsequent procedures for proteolytic digestion, partial acid hydrolysis, and two-dimensional separation of phosphoamino acids on 20 × 20-cm cellulose TLC plates, are those of Cooper et al. (5).

Quantitative [^{125}I]mAb-binding Studies

A procedure was established to quantify competitive and saturable binding of radiolabeled mAbs to samples of liver and MDCK cells immobilized on nitrocellulose paper. Monoclonal antibodies R40.40D3 and R40.76 were purified to homogeneity and labeled with [^{125}I]Bolton Hunter reagent ([^{125}I]iodinated *p*-hydroxyphenylpropionic acid *N*-hydroxysuccinimide ester, 2,000 Ci/mmol) by the method suggested by the manufacturer (Amersham Corp.). Typical specific activities by scintillation counting were ~1.5 × 10^5 cpm/μg mAb. Labeled antibodies continued to specifically identify ZO-1 on immunoblots and were stored in 2 mg/ml BSA, PBS, 0.05% NaN_3. As the antigen source, livers from 4–6-wk-old female cd-1 mice (Charles River Breeding Laboratories, Inc., Willmington, MA) were homogenized in 99 vol (wt/vol) of 1 mM $NaHCO_3$, pH 8.0, containing 2.5 μg/ml leupeptin, 0.5 μg/ml chymostatin and pepstatin, and 0.02 TIU aprotinin. Confluent monolayers of MDCK cells were washed three times in cold PBS containing 0.2 mM PMSF and scraped into the buffer above. Protein from both sources was quickly precipitated by addition of TCA to 5%, collected by centrifugation, and resuspended in 25 mM Tris, pH 8.0, 190 mM glycine, 0.1% SDS at a final concentration of 0.5 mg protein/ml. The number of MDCK cells and linear intercellular junction length per unit area of culture plate were quantified on one half of each of these plates. To make these measurements, cells were fixed and permeabilized on the plate in 100% methanol at −20°C for 1 min, washed three times for 3 min each in PBS, and stained for indirect immunofluorescence microscopy. Cell number per unit area was quantified from photomicrographs of these monolayers stained either with antiZO-1 antibodies, which stains exclusively each cell's junctional perimeter, or with rhodamine-conjugated phalloidin (1:100 in PBS; Molecular Probes, Inc., Junction City, OR), which stains the zonula adherens junctions. Cell perimeter length per unit area of monolayer was determined from these micrographs by tracing with an integrating planimeter (Electronic Graphics Calculator; Numonics Corp., Lansdale, PA).

For quantification of antibody binding, multiple 5-μg aliquots of TCA-precipitated liver or MDCK protein were applied to nitrocellulose paper (Schleicher & Schuell Inc., Keene, NH) using a Hybri-slot manifold (0.5 × 4.0 mm slot orifice; Bethesda Research Laboratories, Gaithersburg, MD). Blocking was done in 5% nonfat dry milk (Carnation Co.)/TBS for 1 h at 37°C. Duplicate samples were incubated in known concentrations of [^{125}I]mAbs in 1 mg/ml BSA, PBS, 0.05% NaN_3, with gentle shaking for 3 h at room temperature. After removing the blots, free mAb concentration was determined by scintillation counting of the incubation solution. Blots were washed twice, 4 min each, in large volumes (500 ml) of incubation buffer without antibody, and then dried. Antibody binding was quantified by integrating the area of densitometry scans on autoradiograms. Standard curves of scanned areas vs. [^{125}I]mAb were constructed by directly blotting known amounts of [^{125}I]mAbs onto nitrocellulose paper and autoradiographing and scanning them in parallel with unknown samples. Based on SDS-PAGE, the molar weight of both mAbs used was 160,400 g/mol (two heavy and two light chains); bound antibody protein was converted to bound moles of antibody using this conversion. Specific binding was determined as that which was competed by simultaneous incubation in a 50- or 100-fold excess of nonradioactive antibody. Preliminary studies showed specific binding was only linear up to ~10 μg/slot of protein; 5 μg/slot was used in all reported studies. Specific mAb binding was analyzed by Scatchard plot analysis.

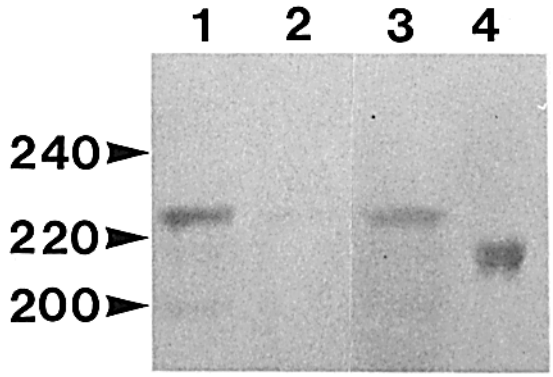

Figure 1. Comparison of apparent molecular masses of ZO-1 by immunoblot analysis. ZO-1–containing samples from the following sources: lane *1*, mouse liver; lane *2*, mouse colonic epithelium; lane *3*, mouse kidney; and lane *4*, MDCK cultured cells. Positions of molecular mass standards are indicated.

Other Methods

Methods for SDS-PAGE, electrophoretic transfer of proteins to nitrocellulose paper, and immunoblot analysis using anti-ZO-1 antibodies have been described in detail (25) and are modifications of the methods of Laemmli (17) and Towbin et al. (27). Molecular mass standards for SDS-PAGE were human RBC spectrin (240 and 220 kD), skeletal muscle myosin (200 kD), beta-galactosidase (116 kD), phosphorylase (92 kD), BSA (68 kD), and ovalbumin (48 kD). Protein determination was done by the method of Hartree (13) or the BCA assay (Pierce Chemical Co., Rockford, IL) using a BSA standard assuming an $OD^{10\ mg/ml}_{280\ nm}$ of 6.7 (9). Autoradiography was done on Kodak X-OMAT AR film at −70°C, using a Lightning Plus-BG intensifying screen (DuPont Co., Wilmington, DE). Liquid scintillation counting of ^{35}S- and ^{125}I-containing samples was done in Optifluor (Packard Instruments Co., Inc., Downers Grove, IL). Standard deviations are presented with *n*, the sample size. Relative ZO-1 content on lanes of the same immunoblots was determined by scanning densitometry in the reflectance mode.

Results

Interspecies Difference in the Molecular Mass of ZO-1

The apparent molecular mass of ZO-1 on immunoblots is 225 kD in samples derived from mouse liver and 210 kD in the MDCK cell line (Fig. 1). This apparent interspecies difference was seen regardless of whether gel samples were taken from whole tissue or from purified membranes, making proteolysis an unlikely explanation for the difference. This is not an interorgan (i.e., isoform) difference since the molecular mass of ZO-1 in samples derived from mouse liver, kidney, colon, and stomach were the same (stomach data not shown).

ZO-1 Is a Peripherally-associated Membrane Protein

Previous immunoelectron microscopic localization using isolated liver plasma membranes demonstrated ZO-1 epitopes on the cytoplasmic surface of the membrane at cell–cell membrane contact points (25). These images, however, do not resolve whether the antigen is a peripheral or integral membrane protein. To investigate this we determined the extrac-

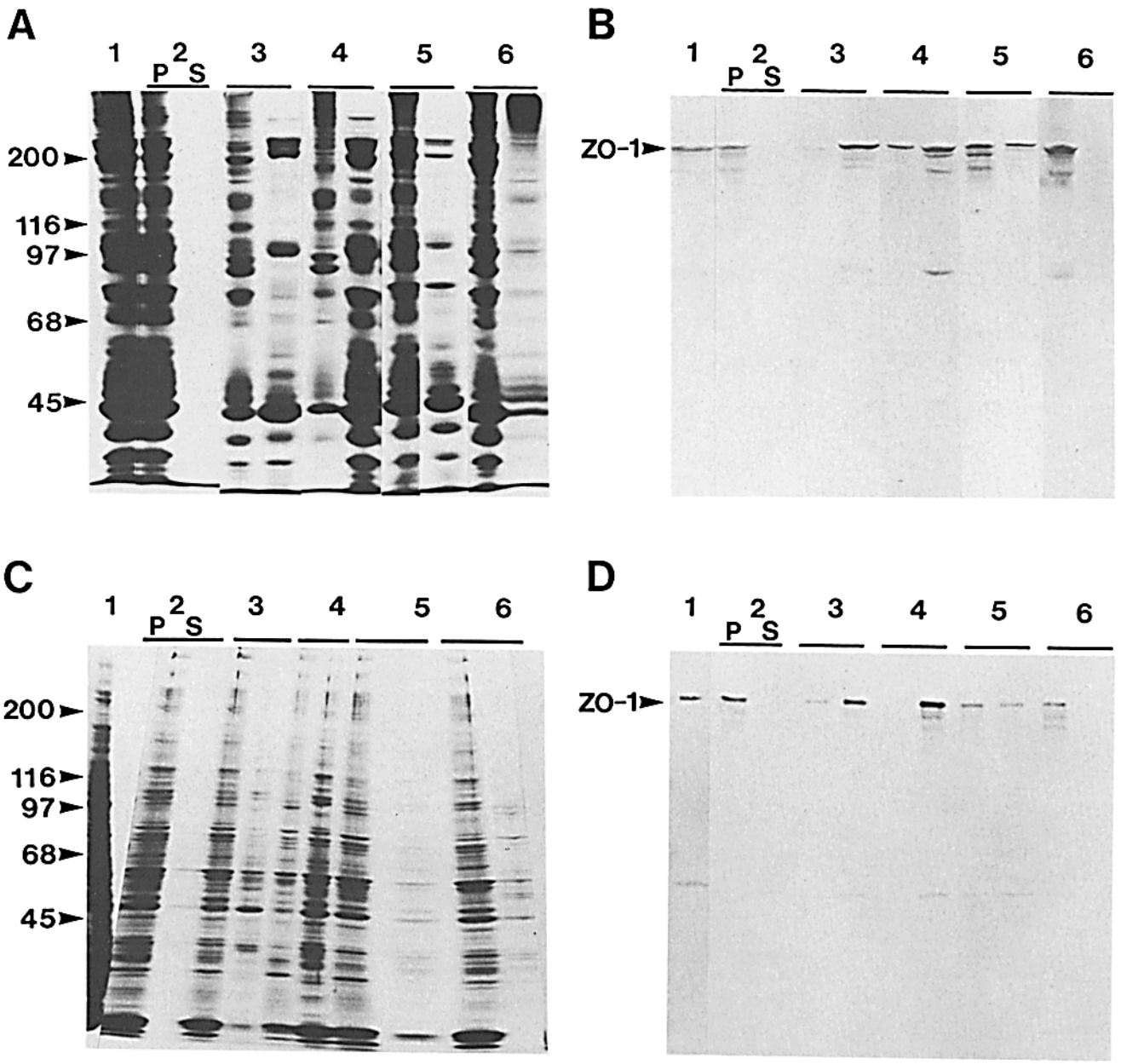

Figure 2. Extraction characteristics of ZO-1 from purified mouse liver (*A* and *B*) and MDCK membranes (*C* and *D*). Coomassie-stained SDS-PAGE (*A* and *C*) and immunoblots of corresponding samples (*B* and *D*) showing proteins and ZO-1 in the pellet (*P*) and supernatant (*S*) after exposure to specified extraction solutions followed by centrifugation at 100,000 *g* for 1 h. Lanes *1*, purified membranes; lanes *2*, exposure to control buffer; lanes *3*, pH 11.0; lanes *4*, 6 M urea; lanes *5*, 0.3 M KCl; lanes *6*, 2% TX-100. See Materials and Methods for details. Positions of molecular mass standards are indicated.

tion characteristics of ZO-1 in purified membranes (Fig. 2) from both liver (Fig. 2, *A* and *B*) and MDCK cells (Fig. 2, *C* and *D*). Most effective solubilization of ZO-1 from liver membranes occurs under denaturing conditions including high pH (pH 11) and 6 M urea (Fig. 2 *B*, lanes *3* and *4*). Both conditions solubilize a similar subset of Coomassie-visible proteins from the membranes (Fig. 2 *A*, lanes *3* and *4*). Release of ZO-1 is almost quantitative with high pH and usually 80–90% with urea, based on densitometric scans of immunoblots. Addition of 1% TX-100 allowed quantitative solubilization of ZO-1 with 6 M urea, suggesting 10–20% may be trapped in closed membrane vesicles (results not shown). Extraction of hepatocyte membranes with 0.3 M KCl (Fig. 2 *B*, lane *5*) released a smaller percent of ZO-1 (never >30%) and frequently promoted extensive proteolysis, despite use of numerous protease inhibitors. KCl, NaCl, and KI in concentrations up to 1 M gave similar results. The nonionic detergents TX-100 (Fig. 2 *B*, lane *6*) or octyl-β-D-glucopyranoside, both at 2%, which typically solubilize integral membrane proteins (29), do not solubilize ZO-1. These extraction characteristics of ZO-1 from purified membrane fractions are typical of a peripherally associated protein. Extraction of ZO-1 from plasma membranes of MDCK cells provided qualitatively identical results (Fig. 2, *C* and *D*). Be-

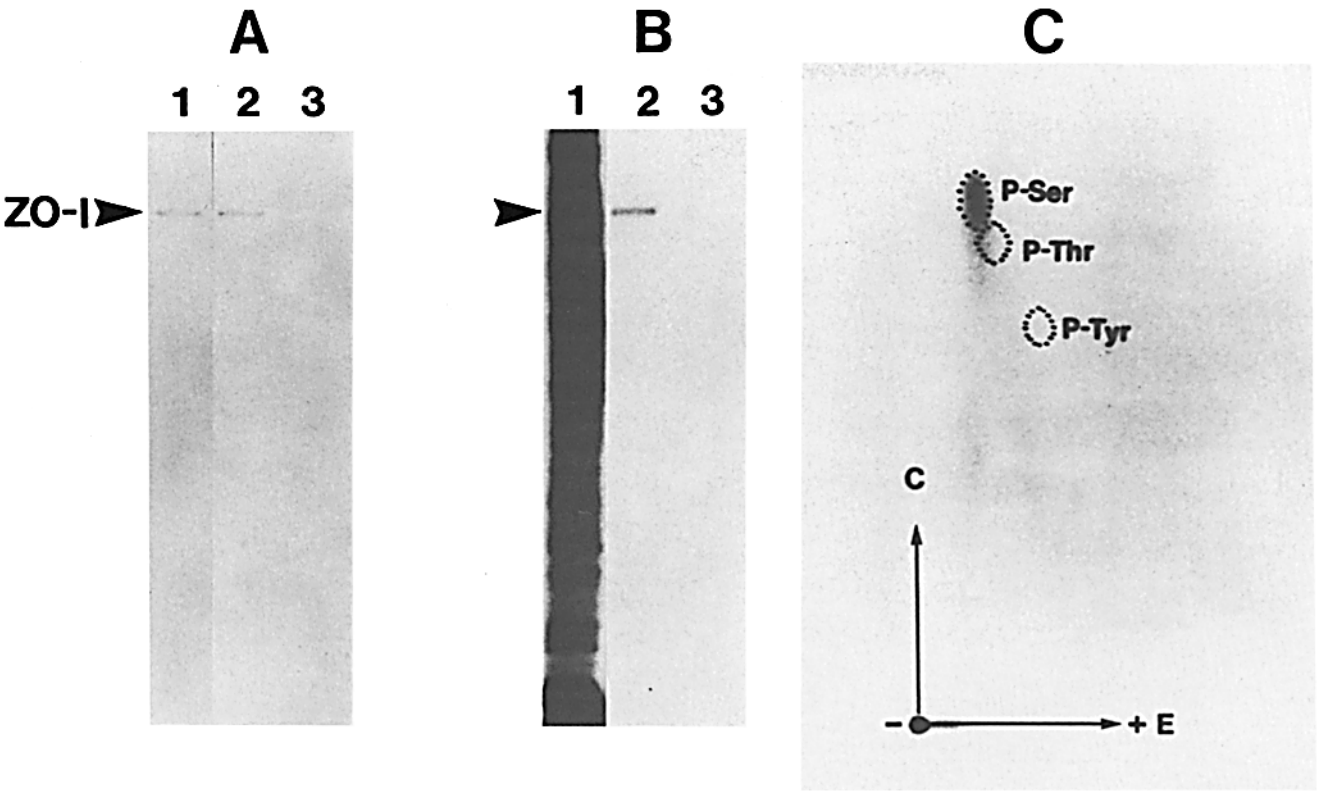

Figure 3. Immunoprecipitation and phosphoamino acid analysis of ZO-1 from [^{32}P]phosphate metabolically labeled MDCK cells. (*A*) Immunoblot and (*B*) corresponding autoradiogram. Lanes *1*, whole cell homogenate; lanes *2*, protein specifically immunoprecipitated with R26.4C-Sepharose; lanes *3*, control precipitate using protein A–Sepharose. Position corresponding to ZO-1 is noted. (*C*) Autoradiograph of [^{32}P]phosphoamino acids contained in immunoprecipitated ZO-1. First dimension electrophoresis (*E*); second dimension chromatography (*C*). Phosphoamino acid standards were cofractionated, located by ninhydrin staining, and their positions outlined. ZO-1 can be selectively immunoprecipitated, is a phosphoprotein, and contains only phosphoserine.

cause nondenaturing extraction conditions proved inefficient and frequently, but not invariably, promoted proteolysis of ZO-1 during subsequent attempts at purification, extraction in urea was routinely used.

Phosphoamino Acid Analysis

ZO-1 is a phosphoprotein as demonstrated in [^{32}P]orthophosphate metabolically labeled MDCK cells (Fig. 3). SDS-PAGE/immunoblot analysis of these cells (Fig. 3 *A*) demonstrates that ZO-1 is present in total soluble protein of MDCK cells (lane *1*), and that ZO-1 can be specifically immunoprecipitated with R26.4C-Sepharose (lane *2*). Autoradiographic analysis (Fig. 3 *B*) demonstrates the presence of many phosphoproteins in MDCK cells (lane *1*) and that ZO-1, which is specifically immunoprecipitated (lane *2*), is also phosphorylated. When [^{32}P]ZO-1 was analyzed for phosphoamino acids by two-dimensional electrophoresis and chromatography, only phosphoserine was detected (Fig. 3 *C*). TCA-precipitable [^{32}P]phosphate had equilibrated at the labeling time used and when the phosphoamino acid profile in whole MDCK cells was analyzed by identical procedures, the typical relative ratios of phosphoserine > phosphothreonine > phosphotyrosine seen in many cell types (5) were detected. It should be noted that cells were not subjected to any specific stimulus to alter kinase activities.

Physical Properties of ZO-1

We attempted preparative purification of ZO-1 from 100-g quantities of mouse liver using a variety of biochemical techniques. However, despite the unique fractionation characteristics of the immunoreactive protein on sucrose gradient centrifugation, gel permeation, ion exchange, and immunoaffinity chromatography, the problems of proteolysis and the very small amounts of ZO-1 present prevented its purification to homogeneity. We were able to purify analytical quantities of ^{35}S-labeled ZO-1 from MDCK cells, where proteolysis is less of a problem, by extracting purified membranes followed by fractionation of solubilized proteins on gel permeation and immunoaffinity chromatography (Fig. 4). When proteins are solubilized from purified membranes in 6 M urea and then fractionated directly by gel chromatography in a buffer without urea, all the immunoreactive ZO-1 elutes as a single discrete peak. ZO-1 present in these column fractions can be quantitatively immunoprecipitated with R26.4C-Sepharose and then released in a soluble form with urea. Immunoaffinity-purified ZO-1 subjected to SDS-PAGE shows a single band of radioactive protein at 210 kD on autoradiograms; no other associated subunits are seen (Fig. 4, lane *8*).

Hydrodynamic characterization of immunoaffinity-purified MDCK ZO-1 was done by gel permeation chromatogra-

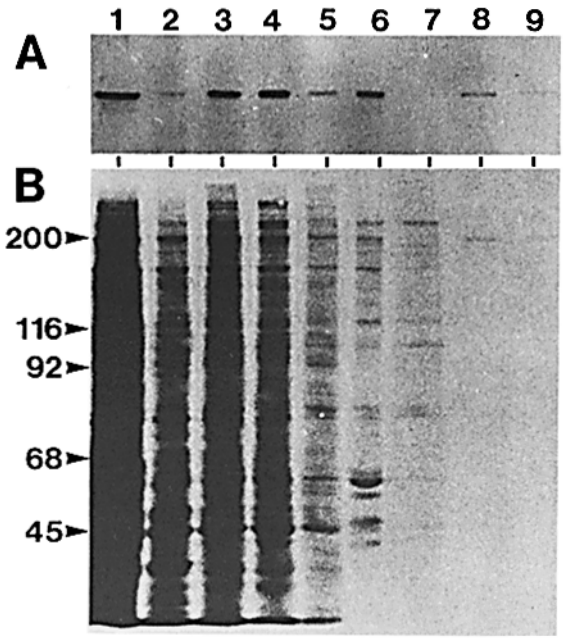

Figure 4. Purification of ZO-1 from ^{35}S-labeled MDCK cells. (*A*) Immunoblot showing ZO-1 in sequential steps of a purification scheme (see Materials and Methods) (*B*) Autoradiogram showing proteins in corresponding samples after SDS-PAGE. Lane *1*, homogenized MDCK cells; lane *2*, low speed supernatant of homogenized cells; lane *3*, low speed pellet of homogenized cells; lane *4*, 6 M urea extract of sucrose gradient–purified membranes; lane *5*, urea-extracted membrane pellet; lane *6*, peak ZO-1–containing fraction from S-400 gel chromatography of urea-extracted proteins; lane *7*, post-immunoprecipitate supernatant; lane *8*, ZO-1 immunoprecipitated from peak S-400 fractions; lane *9*, ZO-1 released with urea from immunoaffinity matrix and used for hydrodynamic characterization shown in Figs. 5 and 6. Positions of molecular mass standards are indicated.

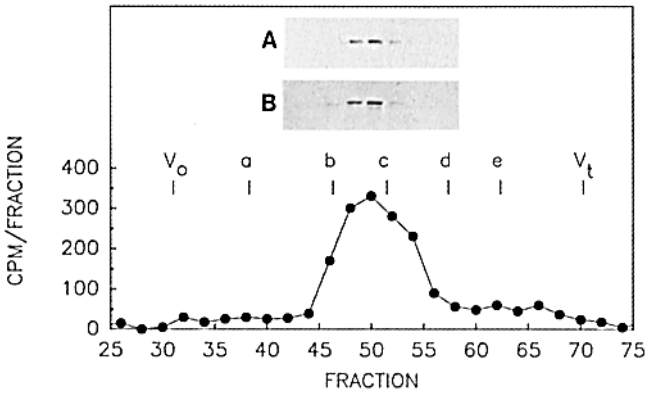

Figure 5. Estimation of the Stokes radius of ZO-1 by gel filtration chromatography. ^{35}S-labeled ZO-1 was purified by immunoprecipitation and after fractionation on an S-400 column (1.5 × 48.0 cm) located by scintillation counting of whole column fractions. Elution positions of marker proteins are indicated: (*a*) human spectrin tetramer (19.4 nm); (*b*) human spectrin dimer (12.3 nm); (*c*) thyroglobulin (8.5 nm); (*d*) ferritin (6.1 nm); (*e*) catalase (5.2 nm). Void volume (V_o) and column-included volume (V_t) are indicated. (*Inset A*) Immunoblot of fractions of ZO-1 chromatographed after extraction from membranes with 0.3 M KCl. (*Inset B*) Immunoblot of fractions of ZO-1 extracted in 6 M urea.

phy (Fig. 5) and sucrose gradient centrifugation (Fig. 6). The elution position of ^{35}S-labeled ZO-1 (Fig. 5) is the same as ZO-1 extracted from purified membranes into either 0.3 M KCl (Fig. 5, *inset A*) or 6 M urea (Fig. 5, *inset B*), and loaded directly on the column. Whether purified or in crude extracts, immunoreactive ZO-1 behaves with the same monodisperse profile as the pure marker proteins, implying a single hydrodynamic form. Because solubilization with salt is unlikely to cause denaturation, the similar hydrodynamic behavior of urea-solubilized ZO-1 implies that the probable denaturation occurring during extraction into urea is reversible during chromatography in nondenaturing buffers. The sedimentation of pure ^{35}S-labeled ZO-1 (Fig. 6) is also indistinguishable from ZO-1 extracted in 0.3 M KCl (*inset A*) or 6 M urea (*inset B*). The estimated Stokes radius, 8.6 nm, and $s_{20,w}$, 5.3, obtained by comparison with known standards, permits calculation of an M_r for the soluble form of ZO-1 of 218 kD. This is similar to the polypeptide mass of 210 kD determined on SDS-PAGE. This is consistent with the single polypeptide visualized at 210 kD on autoradiograms of pure ZO-1 and implies ZO-1, under all conditions studied, behaves as a monomer. The calculated frictional coefficient of 2.2 also suggests the structure is quite asymmetric. All measurements of R_a and $s_{20,w}$ were repeated at least three times and varied within ~5%. With an error in this range, an unidentified subunit of up to 10 kD could conceivably be removed without a detectable alteration in hydrodynamic properties.

It was not possible to make the same analytic measurements on purified ZO-1 from mouse liver. The physical characteristics of immunoreactive ZO-1 could, however, be determined in crude protein mixtures. While this does not allow unambiguous determination of subunit composition, the results were very similar to those of MDCK ZO-1. Table I summarizes the physical characteristics of ZO-1; calculated values are consistent with the conclusion that solubilized ZO-1 from both sources is an asymmetric monomer.

Quantification of ZO-1 Epitopes in Liver and MDCK Cells

It became obvious during attempts to purify ZO-1 that it is present at very low levels, as expected from its very limited cellular localization. Because we were not able to purify a measurable amount with known yield and thus establish a tissue content, we developed a radioimmunoassay technique using ^{125}I-labeled mAbs to measure the content of ZO-1 epitopes in whole cell protein immobilized on nitrocellulose (see Materials and Methods for details). It was observed that radiolabeled mAbs showed a saturable binding to immobilized cell protein which could be competed for by nonlabeled antibody. Representative data for the specific binding of the [^{125}I]R40.76 mAb to immobilized samples of whole mouse liver and whole MDCK cells is presented in Fig. 7 *A* (solid symbols). The average of duplicate determinations is plotted. Nonspecific binding has been subtracted and in the case of MDCK protein, was <5% of total binding. Nonspecific binding to whole liver was usually ~30% of the total, making measurements in this tissue less reliable than those from MDCK cells. There was no specific binding to blotted irrelevant proteins, such as BSA, or the protein constituents in

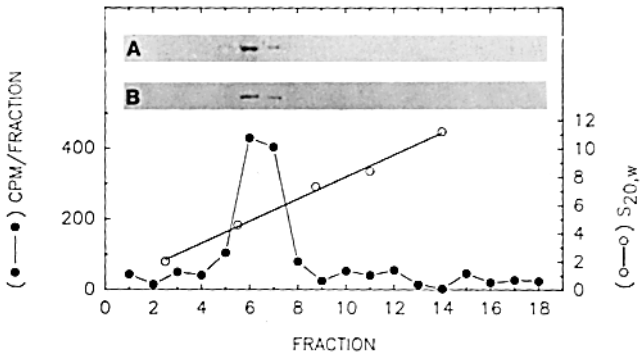

Figure 6. Determination of sedimentation coefficient of ZO-1 by rate-zonal sedimentation. Fractions presented top to bottom, 1–18. ^{35}S-labeled ZO-1 was purified by immunoprecipitation (see Fig. 4) and after centrifugation, its position was located by scintillation counting of whole gradient fractions (●). (*Inset A*) Immunoblot profile of fractions across gradient of proteins extracted from purified MDCK plasma membranes into 0.3 M KCl. (*Inset B*) Immunoblot gradient profile of proteins obtained from ZO-1–containing fractions of an S-400 column (see Fig. 5). Protein applied to the S-400 column had been solubilized in 6 M urea from purified membranes. Positions of markers are plotted (○) vs. their $s_{20,w}$ values and fit by linear least-squares regression. Markers are catalase (11.2), human spectrin (8.4), aldolase (7.3), BSA (4.6), myoglobin (2.0). Note that ZO-1 whether in crude high salt extracts, urea-solubilized and fractionated on S-400, or immunoaffinity-purified sediments with an $s_{20,w}$ of ~5.3.

nonfat dry milk. Scatchard analysis of these data (Fig. 7 *B*) indicates that saturation binding occurs at 60 ng mAb/mg MDCK cell protein and 26 ng/mg liver protein. The apparent binding constants are ~53 nM for MDCK cell and 12 nM for mouse liver protein. The average saturation binding measured in four confluent culture plates was 63 ± 5.7 ng/mg and in three separate mouse livers was 32 ± 8.0 ng/mg.

Antibody-binding analysis to MDCK protein was duplicated with a second mAb, R40.40D3 (Fig. 7 *A* and *B*, open circles). When radiolabeled mAb binding is measured in the presence of 50-fold excess nonlabeled mAb the R40.40D3 and R40.76 mAbs demonstrate a mutual lack of competition and thus recognize different epitopes. Saturation binding for the R40.40D3 mAb was ~15% higher (n = 2), or within the error of the measurements.

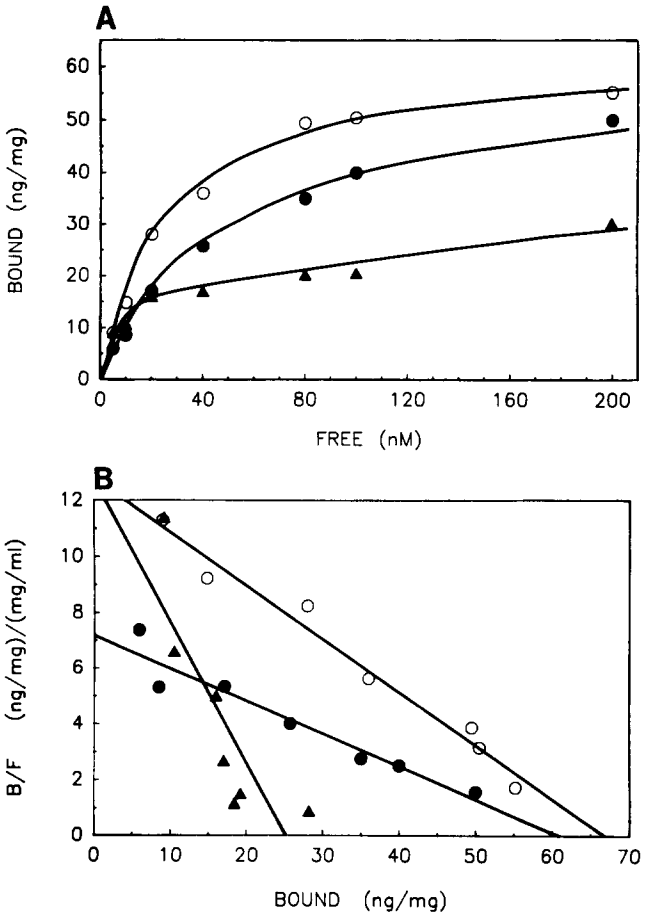

Figure 7. Binding analysis of the [^{125}I]R40.76 and [^{125}I]R40.40D3 mAbs to mouse liver and MDCK cell proteins immobilized on nitrocellulose. (*A*) Specific binding of R40.76 to whole mouse liver proteins (▲) and to MDCK cell proteins (●); specific binding of R40.40D3 to MDCK cell proteins (○). Average of duplicate determinations are expressed as ng of mAb bound per mg of protein vs. free antibody concentration. (*B*) Scatchard plot of the binding data presented in *A*; the same symbols are used. Saturation binding occurs at ~26 ng/mg in liver using the R40.76 mAb and 60 ng/mg in MDCK cells for either the mAb. For the R40.76 mAb the apparent binding constant is ~12 nM for mouse liver and 53 nM for MDCK cells.

Table I. Summary of Physical Properties of ZO-1 from MDCK Cells and Mouse Liver

Property	Value	
	MDCK ZO-1	Mouse liver ZO-1
$s_{20,w}$	5.3	6.0
R_a	8.6 nm	9.0 nm
M_r*	218,000	248,400
Frictional ratio (f/f_o)*	2.2	2.3
M_r (SDS electrophoresis)	210,000	225,000

* Calculated from equations:

$$M_r = \frac{6\pi N R_a s_{20,w}}{1 - v\rho_{20,w}}$$

and

$$f/f_o = R_a\left(\frac{4\pi N}{3M_r\,(v + \delta\rho)}\right)^{1/3},$$

where v and δ were assumed to be those of average soluble proteins, 0.73 cm^3/g and 0.2 g of solvent/g of protein (26). $N = 6.02 \times 10^{23}$.

Although knowledge of the apparent affinities is not necessary to establish epitope content, it is interesting that the affinity of the R40.76 antibody for ZO-1 is over four times higher in the species originally used as the immunogen. As measured by this assay, the binding of R40.76 to ZO-1 in the human colonic adenocarcinoma cell line, HT-29, was an order of magnitude lower in affinity than to mouse ZO-1, possibly explaining our inability to detect ZO-1 by immunofluorescent staining in these cells (data not shown).

The relationship between ZO-1 epitope content, cell number, and junctional perimeter length/cell were defined for the MDCK monolayers by quantifying ZO-1 from one half of each culture plate and staining the other half with either rhodamine-phalloidin or anti–ZO-1 antibodies. This allowed

simultaneous measurement of cell number and junctional length/cm^2 of monolayer (see Materials and Methods). For MDCK type II cells, grown to confluence on plastic, these values were 3.1 ± 0.6 × 10^5 cells/cm^2 of monolayer; 39.4 ± 3.3 μg total cell protein/cm^2 and 13.5 m of junctional length/cm^2. From these values and the saturation-binding level of the R40.76 mAb there are ~30,000 ZO-1 epitopes/cell or 690 ZO-1 epitopes/μm of junctional perimeter.

Discussion

We have presented a description of the physical and biochemical characteristics of the tight junction–associated protein ZO-1 in mouse liver and in the MDCK cell culture line. Aside from the small apparent interspecies difference in polypeptide mass, ZO-1 from both sources appears to be a large, asymmetric, monomeric phosphoprotein tightly associated with the junction as a peripheral membrane protein. Previous immunogold labeling studies (25) demonstrated ZO-1 to be concentrated at the points of cell–cell contact that correspond to fibrils observed in freeze-fracture electron microscopy.

ZO-1 solubilized with denaturing concentrations of urea showed only limited proteolysis, and its yield was greatly increased compared with extraction into 0.3 M KCl. It regained its native hydrodynamic characteristics during subsequent gel chromatography in non-urea–containing buffers and also after purification to homogeneity by an immunoaffinity matrix. Under the solubilization conditions used here, we find no evidence for association with nonidentical subunits or for ZO-1 oligomerization. However, it is clear that ZO-1 is tightly associated with other membrane components and requires nonphysiologic conditions for efficient solubilization, thus we cannot rule out the possibility that ZO-1 associates with either itself or additional subunits in the cell.

ZO-1 is present at low levels. To estimate its cellular content, a quantitative radioimmunoassay was developed using cell protein immobilized on nitrocellulose. To convert measurements of mAb binding per cell protein into an estimate of the actual number of ZO-1 molecules per cell, several assumptions must be made. (*a*) An mAb is bound to every epitope at the measured saturation binding levels; (*b*) each potentially bivalent mAb binds only one epitope; (*c*) all epitopes are accessible; and (*d*) there is only one epitope per ZO-1 molecule. This last assumption is likely to be correct since two different mAbs saturate at the same level. Some of these assumptions, however, are not testable without a purified antigen standard. As a synthetic standard we have produced and measured mAb binding to a recombinant β-galactosidase fusion protein that is recognized by five separate anti–ZO-1 mAbs. The cDNA coding for this putative fragment of ZO-1 was originally identified by screening a rat kidney–derived cDNA expression library in lambda-gtll with the anti–ZO-1 antibodies. Two different rabbit polyclonal antisera to this fusion protein identify only ZO-1 on immunoblots and exclusively stain the junctional complex by immunofluorescence (unpublished results). In the immobilized antigen assay, the R40.76 mAb binding saturates at 0.78 mol mAb/mol fusion protein, suggesting the other assumptions above are approximately correct.

The measurements presented suggest there are ~30,000 copies of ZO-1 per MDCK cell, or ~700 ZO-1 molecules/μm of junctional length. This number can be compared to the number of fibril particles in published freeze-fracture images of MDCK tight junctions. Images produced by Gonzales-Mariscal et al. (12), where cells were grown under identical conditions, demonstrate that fibrils are composed of rows of intramembrane particles. As noted by these authors, the fibril pattern in cultured MDCK is very irregular, varying abruptly between 1 and 10 strands, unlike the regularity observed in epithelia in situ. However, they determined there is an average of four circumferential fibrils and by inspection of their micrographs, which reveal ~120 intramembrane particles/μm of fibril length, we derive 480 intramembrane particles/μm of junctional length. Thus, the molecules of ZO-1, a peripheral protein, and the fibril particles, perhaps representing integral protein component(s) of the junction, appear to be present in very similar amounts.

Although the function of the ZO-1 is unknown, the results presented here have helped define some of the possibilities. As a peripheral protein on the cytoplasmic surface of the tight junction, it clearly is not an integral membrane protein responsible for the freeze-fracture fibrils. However, the close apposition of the ZO-1 to points of membrane contact (i.e., fibril sites) and the similarity between the number of ZO-1 molecules and fibril particles certainly suggests that this protein could interact directly with the (presumed) integral membrane protein(s) of the fibril. For example, ZO-1 might interconnect molecules within a fibril or link fibril molecules to cytoskeletal elements of the cytoplasm. It is unlikely, however, that ZO-1 functions to link fibrils together at branch sites since it is present in Sertoli cell junctions (25) where fibril–fibril anastamoses are rare. Alternatively, ZO-1 might not bind directly to the fibrils, but rather could be one element of a complex assembly of proteins on the cytoplasmic surface of the tight junction, perhaps analogous to the plaques found in association with adherens junctions or desmosomes (14, 15). Unlike these junctions, however, the tight junction has no extensive plaque structures when viewed by conventional electron microscopy.

The observation that ZO-1 is a phosphoprotein raises the question of whether this modification has functional significance. One possibility would be that phosphorylation changes could modify ZO-1 affinity for another protein in the junction complex or modify an unknown enzymatic activity of the protein. There exists numerous examples of hormonal agonists or drugs affecting known kinase systems with coincident alteration of tight junction morphology and paracellular permeability (7, 16, 20, 21). However, whether such coincidental phenomena are of actual physiologic relevance is not resolved. Correlation of ZO-1 phosphorylation levels with functional states of the tight junction may shed light on this problem and the physiologically important problem of the molecular basis of how tissue-specific tight junction function is generated.

We thank Dr. C. M. Van Itallie and members of the Mooseker laboratory for helpful discussions, and D. Babasick and D. Sliker for technical assistance.

This work was supported by grants from the National Institutes of Health to Mark S. Mooseker (GM37556) and Daniel A. Goodenough (GM-28932), and by a Liver Center Grant (J. L. Boyer, Director) Pilot Project (DK 34989). James Melvin Anderson is supported by a National Research Service Award (DK-07864) and the Terry Kirgo Memorial Fellowship from the American Liver Foundation.

Received for publication 3 November 1987, and in revised form 22 December 1987.

References

1. Ackers, G. K. 1970. Analytical gel chromatography of proteins. *Adv. Protein Chem.* 24:343–446.
2. Balcarova-Stander, J., S. E. Pfeiffer, S. D. Fuller, and K. Simons. 1984. Development of cell surface polarity in the epithelial Madin-Darby canine kidney (MDCK) cell line. *EMBO (Eur. Mol. Biol. Organ.) J.* 3:2687–2694.
3. Cereijido, M., E. S. Robbins, W. J. Dolan, C. A. Rkotunno, and D. D. Sabatini. 1978. Polarized monolayers formed by epithelial cells on a permeable and translucent support. *J. Cell Biol.* 77:853–880.
4. Claude, P., and D. A. Goodenough. 1973. Fracture faces of zonulae occludentes from "tight" and "leaky" epithelia. *J. Cell Biol.* 58:390–400.
5. Cooper, J. A., B. M. Sefton, and T. Hunter. 1983. Determination and quantitation of phosphotyrosine in proteins. *Methods Enzymol.* 99:387–402.
6. Diamond, J. M. 1977. The epithelial junction: bridge, gate and fence. *Physiologist.* 20:10–18.
7. Duffey, M. E., B. Hainau, S. Ho, and C. J. Bentzel. 1981. Regulation of epithelial tight junction permeability by cyclic AMP. *Nature (Lond.).* 294:451–453.
8. Farquhar, M. G., and G. E. Palade. 1963. Junctional complexes in various epithelia. *J. Cell Biol.* 17:375–412.
9. Foster, J. F., and J. T. Yang. 1954. On the mode of interaction of surface active cations with ovalbumin and bovine plasma albumin. *J. Am. Chem. Soc.* 76:1015–1019.
10. Friend, D. S., and N. B. Gilula. 1972. Variation in tight and gap junctions in mammalian tissues. *J. Cell Biol.* 53:758–776.
11. Galfre, G., and C. Milstein. 1981. Preparation of monoclonal antibodies: strategies and procedures. *Methods Enzymol.* 73:1–45.
12. Gonzalez-Mariscal, L., B. Chavez de Ramirez, and M. Cereijido. 1985. Tight junction formation in cultured epithelial cells (MDCK). *J. Membr. Biol.* 86:113–125.
13. Hartree, E. F. 1972. Determination of protein: a modification of the Lowry method that gives a linear response. *Anal. Biochem.* 48:422–435.
14. Horwitz, A., K. Duggan, C. Buck, M. Beckerle, and K. Burridge. 1986. Interaction of plasma membrane fibronectin receptor with talin-a transmembrane linkage. *Nature (Lond.).* 320:531–533.
15. Jones, J. C. R., and R. D. Goldman. 1985. Intermediate filaments and the initiation of desmosome assembly. *J. Cell Biol.* 101:506–517.
16. Kuiypers, G. A. J., I. G. P. Van Nooy, M. E. N. Vossene, A. M. Stadhouders, A. M. VanUyen, J. H. M. Depont, and S. L. Bonting. 1985. Tight junctional permeability of the resting and carbachol stimulated exocrine rabbit pancreas. *Histochem. J.* 83:257–264.
17. Laemmli, U. K. 1970. Cleavage of structural proteins during the assembly of the head of bacteriophage T4. *Nature (Lond.).* 227:680–685.
18. Madara, J. L., and K. Dharmsathaphorn. 1985. Occluding junction structure-function relationships in a cultured epithelial monolayer. *J. Cell Biol.* 101:2124–2133.
19. Martin, R. G., and B. N. Ames. 1961. A method for determining the sedimentation behavior of enzymes: application to protein mixtures. *J. Biol. Chem.* 236:1372–1379.
20. Mazariegos, M. R., L. W. Tice, and A. R. Hand. 1984. Alteration of tight junction permeability in the rat parotid gland after isoproterenal stimulation. *J. Cell Biol.* 98:1865–1877.
21. Ojakian, G. K. 1981. Tumor promoter-induced changes in the permeability of epithelial cell tight junctions. *Cell.* 23:95–103.
22. Pisam, M., and P. Ripoche. 1976. Redistribution of surface macromolecules in dissociated epithelial cell. *J. Cell Biol.* 71:907–920.
23. Powell, D. W. 1981. Barrier function of epithelia. *Am. J. Physiol.* 241: G275–G288.
24. Stevenson, B. R., and D. A. Goodenough. 1984. Zonulae occludentes in junctional complex-enriched fractions from mouse liver: preliminary morphological and biochemical characterization. *J. Cell Biol.* 98:1209–1221.
25. Stevenson, B. R., J. D. Siliciano, M. S. Mooseker, and D. A. Goodenough. 1986. Identification of ZO-1: a high molecular weight polypeptide associated with the tight junction (zonula occludens) in a variety of epithelia. *J. Cell Biol.* 103:755–766.
26. Tanford, C. 1961. Physical Chemistry of Macromolecules. John Wiley and Sons, New York. 364–396.
27. Towbin, H., T. Staehelin, and J. Gordon. 1979. Electrophoretic transfer of protein from polyacrylamide gels to nitrocellulose sheets: a procedure and some applications. *Proc. Natl. Acad. Sci. USA.* 76:4350–4354.
28. Van Meer, G., and K. Simons. 1986. The function of tight junctions in maintaining differences in lipid composition between the apical and the basolateral cell surface domains of MDCK cells. *EMBO (Eur. Mol. Biol. Organ.) J.* 5:1455–1464.
29. Van Renwoude, J., and C. Kempf. 1984. Purification of integral membrane proteins. *Methods Enzymol.* 104:329–339.
30. Vega-Sales, D. E., P. J. I. Salas, D. Gunderson, and E. Rodriguez-Boulan. 1987. Formation of the apical pole of epithelial MDCK cells: polarity of an apical protein is independent of tight junctions while segregation of a basolateral marker requires cell-cell interactions. *J. Cell Biol.* 104: 905–916.